# Highly enhanced broadband infrared absorption of germanium by multi-layer plasmonic nano-antenna

**Xiaolan Zhong (钟晓岚)[1,2], Ju Liu (刘 菊)[1], and Zhiyuan Li (李志远)[1*]**

[1]*Laboratory of Optical Physics, Institute of Physics, Chinese Academy of Sciences, Beijing 100190, China*

[2]*Department of Electrical and Computer Engineering, National University of Singapore, 4 Engineering Drive 3, Singapore 117576, Singapore*

[*]*Corresponding author: lizy@aphy.iphy.ac.cn*

Received April 11, 2014; accepted May 20, 2014; posted online August 22, 2014

High-sensitivity and broad bandwidth photo-detector devices are important for both fundamental studies and high-technology applications. Here, by using three-dimensional (3D) finite-difference time-domain simulation, we design an optimized 3D multi-layer gold nano-antenna to enhance the near-infrared (NIR) absorption of germanium nanoparticles. The key ingredient is the simultaneous presence of multiple plasmonic resonance modes with strong light-harvesting effect that encompass a broad bandwidth of germanium absorption band. The simulation results show more than two orders of magnitude enhanced absorption efficiency of germanium around 1550 nm. The design opens up a promising way to build high-sensitivity and broad bandwidth NIR photo-detectors.

*OCIS codes: 240.6680, 230.5750, 220.2740, 290.5850.*

*doi: 10.3788/COL201412.092401.*

Photonic nanomaterial, in particular plasmonic nano-antenna, enables enhancement of light–matter interaction at nanoscale that can be harnessed to build high-performance optoelectronic devices[1–4]. There is significant interest in developing high-sensitivity, broad bandwidth, and power efficient photonic detection devices that are composed of direct bandgap semiconductors, such as III–V[5–9] and IV semiconductors[10–13]. Germanium has been assumed as the most promising candidate material to build the high-sensitivity near-infrared (NIR) photonic detector[14–20] because of its direct gap of 0.8 eV[10,13], which corresponds to the most technically important telecommunications wavelength of 1550 nm. However, previous studies were so far not very effective in lifting the bottleneck of low absorption of germanium at telecommunication wavelength (which goes beyond the direct bandgap absorption edge of germanium) due to the intrinsic absorption limitation of pure germanium material, although many efforts have been made to enhance the absorption of germanium by using different nanostructures, such as thin film[10] and resonant cavity incorporated waveguide[11].

The absorption cross section of germanium material is an important quantity which measures the performance of photonic devices, such as photonic detectors and absorbers. Efficiently increasing the absorption cross section can be very useful to improve the device performance, and it has been well known that metal nanostructures can be a good solution for this purpose[21–28]. When light interacts with metal nanostructures, surface plasmon resonance can occur and induce huge enhancement of local electromagnetic field either through the lightening rod effect[27] or via the light-harvesting effect in the visible and NIR range[29]. The light-harvesting effect can create "hot spots" of optical field within the vicinity of plasmonic nanostructures, for instance, within the tiny gap of plasmonic nano-antenna[30,31] In our previous work, a giant enhancement of near-ultraviolet light absorption by $TiO_2$ via a three-dimensional (3D) aluminum plasmonic nanofunnel-antenna[23] was reported. Combining the germanium material with 3D plasmonic nanostructures and considering the light-harvesting effect may lead to a giant enhancement of absorption cross section of germanium and a high-performance Ge-based photonic device at the NIR band. Here we present a 3D multi-layer plasmonic nano-antenna that can significantly enhance the NIR absorption cross section of germanium material. Each basic gold square loop antenna in the nanostructure can resonantly interact with the Ge nanoparticles at independent frequency bands, leading to the giant enhancement of absorption cross section of germanium at NIR wavelength with a broad bandwidth covering the whole telecommunication bands.

Our investigations start from the optical properties of pure Ge nanoparticle, which can afford a clear physical image to help understand why we need to increase the absorption cross section of germanium material in the NIR band. By employing the 3D finite-difference time-domain (FDTD) method[32,33] we calculate the absorption cross section of pure Ge nanoparticle. We use perfectly matched layer as the boundary condition. As shown in Fig. 1(a), the absorption cross section increases with particle size obviously. The edge lengths of

 

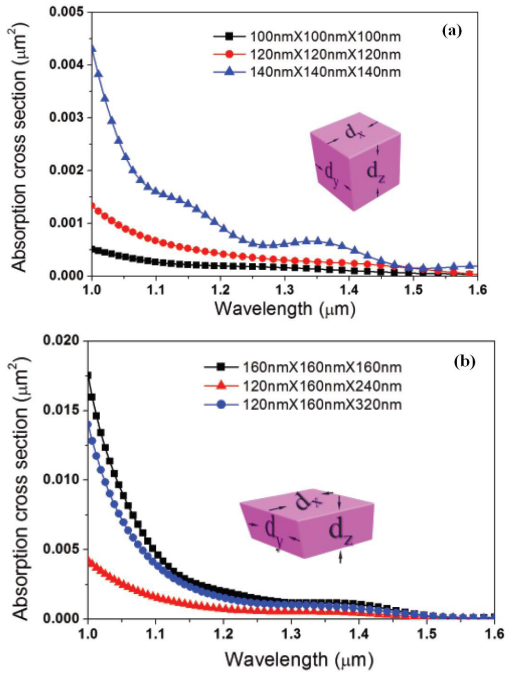


Fig. 1. Absorption cross section of Ge nanoparticle with different sizes: (a) absorption cross section of Ge nanocube calculated using the FDTD method and (b) Ge nanoparticles with the same size embedded in the designed single-, double- and triple-layer gold nano-antenna shown in Fig. 3(a) with different color lines, respectively. Inset: schematic geometry of Ge particle with the edge lengths $d_x$, $d_y$ and $d_z$ along the $x$-, $y$-, and $z$-axes, respectively.

the studied pure Ge nanocube are $d_x$, $d_y$, and $d_z$ along $x$-, $y$-, and $z$-axes, respectively, and the incident plane-wave light propagates along the $z$-axis while polarizes along the $x$-axis. When the wavelength grows, the absorption basically decreases. Remarkably, the absorption cross section is almost close to zero at the telecommunication bands and longer wavelengths. Obviously this originates from the absorptive nature of germanium material in dependence on wavelength.

Plasmonic resonance band due to different nano-antenna structures and their interaction with germanium materials can be controlled by optimizing the plasmonic device. The geometric configurations of the designed multi-layer gold nano-antenna are shown in Figs. 2(a) and (b) for 3D and lateral view, respectively. This structure is composed of three layers of Au square-shape nano-antenna, with the inner layer labeled layer 1, while the outer layers labeled layers 2 and 3, respectively. The Ge nanoparticles are embedded in the central slot of the first layer nano-antenna (particle 1) and in the trench between the first and second layers (particle 2), the second and third layers (particle 3), respectively. The height of each layer is $H_1$, $H_2$, and $H_3$, and the distance between adjacent layers is $D_1$, $D_2$, and $D_3$, respectively, while the thickness of each layer has the same value of $W$. The Ge nanoparticles are embedded inside the slot and their sizes are slightly

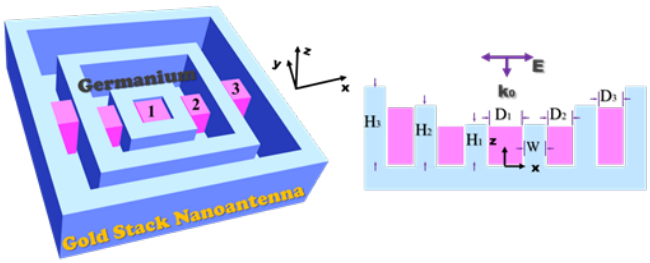


(a) (b)

Fig. 2. Schematic plot of the 3D designed multi-layer plasmonic nano-antenna embedded with germanium nanoparticles: (a) geometry of the plasmonic nano-antenna, which is composed by three gold nano-antenna and germanium nanoparticles embedded inside the antenna tiny gap and (b) lateral view of the nanostructure at $y = 0$.

smaller than the slot with 10 nm shorter in each edge. The origin of coordinates is chosen such that $x = 0$ and $y = 0$ is located at the center of particle 1 while $z = 0$ is 10 nm below the bottom surface of particle 1. $X$- and $y$-axes are parallel to the square edges of the nano-antenna. The most important advantage of this optimized nano-antenna can be summarized follows: due to the irregularly design with triple layers of Au, the nano-antenna can exhibit multiple plasmonic resonance bands, and this allows for strongly enhanced interaction of light with the embedded Ge nanoparticles, leading to greatly enhanced broadband NIR absorption by germanium materials.

We examine the performance of designed multi-layer nano-antenna. Figure 3(a) shows the spectrum of absorption cross section of the three Ge nanoparticles. Through extensive calculation, we find that the influence of the outer Ge particle on the absorption cross section of the inner one is weak. It means all the particles within different locations are independent of each other. Thus we can focus on the absorption properties of each Ge nanoparticle in different cases. The geometric parameters in Fig. 3 are chosen as $D_1 = 180$ nm, $D_2 = 140$ nm, $D_3 = 140$ nm, $H_1 = 180$ nm, $H_2 = 260$ nm, and $H_3 = 340$ nm. These optimized values have been obtained via a large number of numerical calculations and they make the resonance band of absorption cross section of Ge nanoparticle cover the whole telecommunication bands as much as possible. Figure 3(a) shows that the maximum absorption cross section of the central Ge particle (particle 1) takes place at $\lambda = 1100$ nm with $D_1 = 180$ nm and $H_1 = 180$ nm. To better describe the enhancement of germanium absorption cross section, we define a parameter named the enhancement factor of absorption cross section, which is equal to the ratio of the absorption cross section of an embedded Ge nanoparticle over that of a pure Ge nanoparticle. The results for pure Ge nanoparticles whose geometric parameters are the same as those in Fig. 3 are displayed in Fig. 1(b). Observing the spectrum for particle 2 in Fig. 3(a), we find an exciting

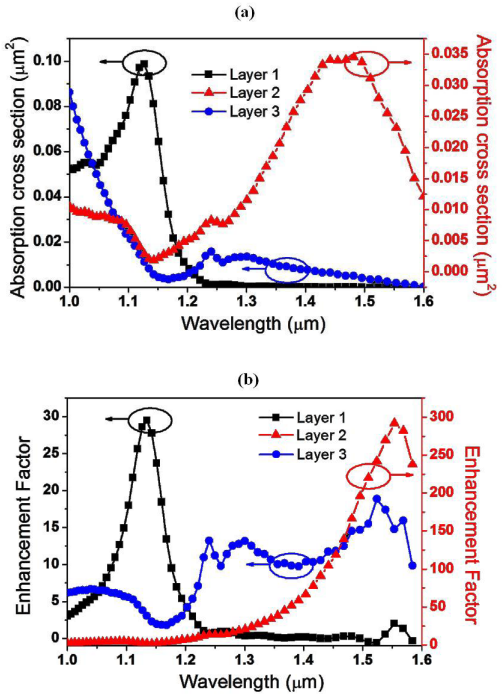


Fig. 3. (a) Absorption cross section of Ge particle embedded in the single-, double-, and triple-layer plasmonic nano-antenna. The geometric parameters here are $D_1 = 180$ nm and $H_1 = 180$ nm for the first layer, $D_2 = 140$ nm and $H_2 = 260$ nm for the second layer, and $D_3 = 140$ nm and $H_3 = 340$ nm for the third layer, respectively. (b) Enhancement factor of absorption, which equals absorption cross section of Ge particle embedded in the single-, double-, and triple-layer plasmonic nano-antenna over the absorption cross section of pure Ge particle.

thing: the absorption efficiency around the telecommunication bands exhibits a giant enhancement (about two orders of magnitude) and the maximum absorption cross section of Ge nanoparticle moves to ~1550 nm. What is more, the maximum enhanced absorption spectrum of particle 3 has an obvious red-shift and broadens to almost cover the whole finite calculation bands. Recalling the independent nature of nanoparticles at different locations, the combination spectra shown in Figs. 3(a) and (b) clearly exhibit a giant magnification of absolute absorption cross section for the Ge nanoparticle. At the same time, the combination spectra illustrate a whole-cover broad bandwidth performance of optical absorption around the NIR bands, especially the telecommunication bands.

It would be helpful to say some words about the design process to find the above-optimized multi-layer nano-antenna by means of the FDTD method. The design process starts from the single-layer Au nano-antenna, named layer 1, and both the edge length and height of the nano-antenna can be changed. When one parameter is changed, the other one should be fixed temporarily. Finally, we obtain the optimized nano-antenna with $D_1 = 180$ nm and $H_1 = 180$ nm, which corresponds to the maximum enhancement of absorption of the central Ge particle (particle 1) at $\lambda = 1100$ nm in Fig. 3(a). Then, we introduce the double-layer structure to further increase the absorption cross section of Ge particles at the telecommunication bands. We fix the optimized geometric parameters of layer 1 as we mentioned above and then adjust the parameters of layer 2 in order to make progress in pushing the maximum absorption cross section wavelength toward the target band. After we get the maximum enhancement of absorption of particle 2 at ~1550 nm, which corresponds to parameters of $D_2 = 140$ nm and $H_2 = 260$ nm, we further introduce the triple-layer structure and find the optimized parameters as $D_3 = 140$ nm and $H_3 = 340$ nm. At this step, the most optimized geometric structures of multi-layer nano-antenna have been found, as shown in Figs. 2(a) and (b).

To better understand the physics behind the broadband NIR absorption by the multi-layer nano-antenna, the electric field intensity distributions are calculated and shown in Fig. 4 for the single-, double-, and triple-layer plasmonic nano-antenna, respectively. The field patterns shown in Figs. 4(a)–(c) correspond to the single, double-, and triple-geometric configurations, respectively. Again $D_1 = 180$ nm, $D_2 = 140$ nm, $D_3 = 140$ nm, $H_1 = 180$ nm, $H_2 = 260$ nm, and $H_3 = 340$ nm. The single-layer structure has the maximum absorption at ~1100 nm and the corresponding field patterns are shown in Figs. 4(a) and (d). We can find that there exist a local field enhancement and light-harvesting effect in the gap between Ge nanoparticle and plasmonic nano-antenna. The maximum enhancement factor of field intensity can reach 1500 (Fig. 4(d)). The double-layer structure has the maximum absorption peak at ~1550 nm that matches the telecommunication band. The corresponding electric field intensity patterns are shown in Figs. 4(b) and (e). We can find a giant local field enhancement between the first and second layers due to the light-harvesting effect, which appears in the second slot. In the triple-layer structure,

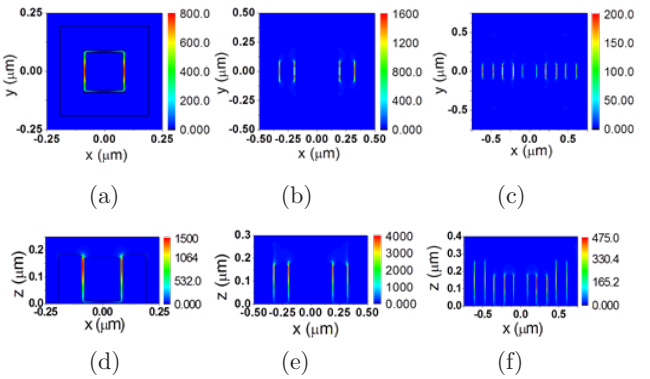


Fig. 4. Top view electric field distributions corresponding to the (a) single-, (b) double-, and (c) triple-layer nano-antenna with $z = 50$ nm, respectively and lateral view electric field distributions corresponding to the (d) single-, (e) double-, and (f) triple-layer nano-antenna, respectively. The black lines in (a) and (d) indicate the nanostructure.

the third layer further enhances the total absorption cross section of Ge nanoparticles and makes the absorption spectrum broader and more efficient.

In conclusion, we present a new method to solve the high-sensitivity and broad bandwidth photonic devices made from Ge nanoparticles embedded in multi-layer plasmonic nano-antenna. By using different positions of Ge nanoparticle in multi-layer structure and the light-harvesting effect, we successfully obtain a high sensitive and broad absorption spectrum with two orders of magnitudes. The giant enhancement of absorption efficiency of Ge nanoparticles by doping into the multi-layer structure suggests an effective method to enhance the absorption of germanium. The 3D multi-layer plasmonic nano-antenna opens up a broad window to design high-sensitivity and broad bandwidth photonic devices.

This work was supported by the National 973 Program of China (No. 2013CB632704) and the National Natural Science Foundation of China (No. 11374357).

## References

1. W. L. Barnes, A. Dereux, and T. W. Ebbesen, Nature **424,** 824 (2003).
2. S. A. Maier, *Plasmonics: Fundamentals and Applications* (Springer, Bath, 2006).
3. J. F. Li and Z. Y. Li, Chin. Phys. B **23,** 047305 (2014).
4. J. F. Li, H. L. Guo, and Z. Y. Li, Photon. Res. **1,** 28 (2013).
5. S. Feng, Y. Geng, K. Lau, and A. Poon, Opt. Lett. **37,** 4035 (2012).
6. P. Yang, R. Yan, and M. Fardy, Nano Lett. **10,** 1529 (2010).
7. S.-H. Wei and A. Zunger, Appl. Phys. Lett. **72,** 2011 (1998).
8. G. V. Naik, V. M. Shalaev, and A. Boltasseva, Adv. Mater. **25,** 3264 (2013).
9. R. Q. Zhang, Y. Lifshitz, and S.-T. Lee, Adv. Mater. **15,** 635 (2003).
10. X. Wang, L. C. Kimerling, J. Michel, and J. Liu, Appl. Phys. Lett. **102,** 131116 (2013).
11. K. C. Balram, R. M. Audet, and D. A. B. Miller, Opt. Express **21,** 10228 (2013).
12. T. Kawase, A. Mura, K. Nishitani, Y. Kawai, K. Kawai, J. Uchikoshi, M. Morita, and K. Arima, J. Appl. Phys. **111,** 126102 (2012).
13. S. Mirabella, S. Cosentino, A. Gentile, G. Nicotra, N. Piluso, L. V. Mercaldo, F. Simone, C. Spinella, and A. Terrasi, Appl. Phys. Lett. **101,** 011911 (2012).
14. S. Cosentino, P. Liu, S. T. Le, S. Lee, D. Paine, A. Zaslavsky, D. Pacifici, S. Mirabella, M. Miritello, I. Crupi, and A. Terrasi, Appl. Phys. Lett. **98,** 221107 (2011).
15. P. Boucaud, V. Le Thanh, S. Sauvage, D. Débarre, and D. Bouchier, Appl. Phys. Lett. **74,** 401 (1999).
16. O. P. Pchelyakov, Y. B. Bolkhovityanov, A. V. Dvurechenski, L. V. Sokolov, A. I. Nikiforov, A. I. Yakimov, and B. Voigtländer, Semiconductors **34,** 1291 (2000).
17. J. Jain, A. Hryciw, and T. Baer, Nat. Photon. **6,** 398 (2012).
18. J. Liu, D. Cannon, and K. Wada, Appl. Phys. Lett. **87**, 011110 (2005).
19. J. Michel, J. Liu, and L. Kimerling, Nat. Photon. **4,** 527 (2010).
20. D. Miller, Proc. IEEE **97,** 1166 (2009).
21. X. L. Zhong and Z. Y. Li, Phys. Rev. B **88,** 085101 (2013).
22. S. Collin, F. Pardo, R. Teissier, and J.-L. Pelouard, Appl. Phys. Lett. **85,** 194 (2004).
23. X. L. Zhong and Z. Y. Li, J. Phys. Chem. C **116,** 21547 (2012).
24. J. Liu, X. L. Zhong, and Z. Y. Li, Chin. Phys. B 23, 047306 (2014).
25. J. Fang, S. Qin, X. Zhang, and S. Chang, Chin. Opt. Lett. **10,** 031601 (2012).
26. Z. Liu, H. Zhong, Z. Guo, and B. Yang, Chin. Opt. Lett. **11,** 083001 (2013).
27. C. D'Andrea, J. Bochterle, and A. Toma, ACS Nano **7,** 3522 (2013).
28. F. Yi, H. Zhu, J. C. Reed, and E. Cubukcu, Nano Lett. **13,** 1638 (2013).
29. M. Borgstrom and J. Wallentin, IEEE J. Select. Top. Quant. Electron. **17,** 1050 (2011).
30. J. Y. Suh, M. D. Huntington, C. H. Kim, W. Zhou, M. R. Wasielewski, and T. W. Odom, Nano Lett. **12,** 269 (2012).
31. Z. Zhang, A. Weber-Bargioni, S. W. Wu, S. Dhuey, S. Cabrini, and P. J. Schuck, Nano Lett. **9,** 4505 (2009).
32. Z. Y. Li and Y. N. Xia, Nano Lett. 10, 243 (2010).
33. J. Goodman, B. Draine, and P. Flatau, Opt. Lett. **16,** 1198 (1991).